Published in *Journal of Physics Conf. Series* (*SuST*) **234**, 032017 (2010)

Progress on the Superconducting Magnets for the MICE Cooling Channel

M. A. Green[a], S. P. Virostek[a], D. Li[a], M. S. Zisman[a], L. Wang[b], H. Pan[b], H. Wu[b], X. L. Guo[b], F. Y. Xu[b], X. K. Liu, S. X. Zheng[b], T. Bradshaw[c], D. E. Baynham[c], J. Cobb[d], W. Lau[d], P. Lau[d], and S. Q. Yang[d],

a) Lawrence Berkeley National Laboratory, Berkeley CA 94720, USA
b) Institute of Cryogenic and Superconductivity Technology, HIT, Harbin, China
c) Rutherford Appleton Laboratory, Chilton Didcot OX11-0QX, UK
d) Physics Department Design Office, Oxford University, Oxford OX1-3RH, UK

Corresponding Author: Michael A. Green at magreen@lbl.gov

Abstract. The muon ionization cooling experiment (MICE) consists of a target, a beam line, a pion decay channel, the MICE cooling channel. Superconducting magnets are used in the pion decay channel and the MICE cooling channel. This report describes the MICE cooling channel magnets and the progress in the design and fabrication of these magnets. The MICE cooling channel consists of three types of superconducting solenoids; the spectrometer solenoids, the coupling solenoids and the focusing solenoids. The three types of magnets are being fabricated in the United States, China, and the United Kingdom respectively. The spectrometer magnets are used to analyze the muon beam before and after muon cooling. The coupling magnets couple the focusing sections and keep the muon beam contained within the iris of the RF cavities that are used to recover the muon momentum lost during ionization cooling. The focusing magnets focus the muon beam in the center of a liquid hydrogen absorber. The first of the cooling channel magnets will be operational in MICE in the spring of 2010.

1. Introduction to the MICE Cooling Channel

The next generation of particle physics accelerators will involve the acceleration and collision of high-energy leptons. There are limits on how much the lowest mass stable lepton (electrons and positrons with a rest mass of 0.51 MeV) can be bent in a magnetic field. The next lowest mass lepton is the muon (rest mass ~100 MeV). High-energy muons can be bent without the synchrotron radiation that comes from bending electrons or positrons.

Muons are produced from the decay of pions, which are produced when protons collide with a fixed target. Muons produced this way have a high emittance. The development of a neutrino factory or a muon collider requires that muon-beams be cooled (reducing their emittance by removing the transverse momentum while retaining the momentum in the direction of the beam). Because a muon has a short lifetime (~2.1 μs at rest), the methods used for cooling positrons and anti protons cannot be employed. The only method that can be applied that will cool muons within their lifetime is ionization cooling. Demonstrating muon ionization cooling is essential to the development of muon accelerators and storage rings [1], [2]. The muon ionization cooling experiment (MICE) is designed to demonstrate muon cooling in a magnet configuration that is useful for a neutrino factory [3], [4].

Muon ionization cooling involves having the muons pass through mass. In doing so, the muon losses momentum in both the longitudinal and the transverse directions. The muons are then accelerated with RF cavities to restore their longitudinal momentum. If the transverse momentum removed by the mass is greater than the transverse momentum put into the muon by scattering off of the cooling medium, beam cooling will result. The cooling medium that results in the best cooling is hydrogen. As a result, it is desirable to use hydrogen (as a liquid or a compressed gas) as an absorber.

The experiment starts with a target that scrapes the halo of the beam at ISIS (a proton accelerator at the Rutherford Appleton Lab). Pions are produced at the target. Some of these pions are captured by the beam line upstream from the pion decay channel. Pions have a lifetime of ~20 ns at rest. Most of the pions will decay into muons in a distance of about 5 meters. The pions and resulting muons are captured within the 100 mm bore of a solenoid that generates a magnetic induction of 5 T.

All of the magnets in MICE are superconducting except for the beam line dipoles and quadrupoles that bend and focus the beam from the target to the MICE cooling channel. There are four types of superconducting solenoid magnets in MICE. They are the 5 T pion decay solenoid (not discussed here) [5] and the three types of solenoid magnets that are in the MICE cooling channel.

The full MICE cooling channel consists of seven magnet modules that contain a total of eighteen superconducting coils. The three types of MICE cooling channel magnet modules are the spectrometer module, the RF coupling coil (RFCC) module, and the absorber focus coil (AFC) module. In the final version of MICE, there are two spectrometer modules, two RFCC modules, and three AFC modules. The experiment will be operated in stages. Each stage will have a different number of magnet modules in it. During stage-2, there will be a single spectrometer module. During stage-3, there will be two spectrometer modules with a solid absorber between them. During stage-4, MICE will operate with two spectrometer modules and a single AFC module that can have either a liquid or a solid absorber within it. Stage-5 has two spectrometer modules, two AFC modules, and a single RFCC module. Stage-6, the final stage, has all seven magnet-modules. Figure 1 shows the MICE cooling channel during final stage of the experiment. Whether the experiment operates at stage-6 with all three AFC modules depends on the funding from the UK for the experiment.

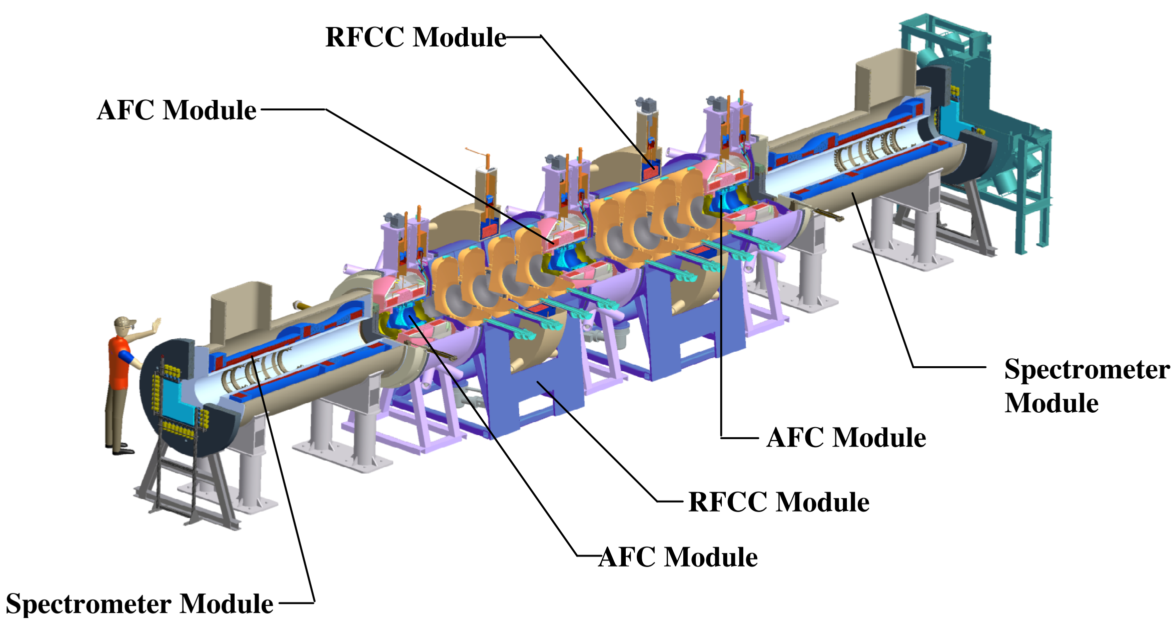

Figure 1. A cross-section view of the MICE cooling channel showing the magnet coils, liquid absorber, RF cavities, and the trackers.

The magnets in the MICE cooling channel have no iron shield. There is an iron wall that shields the ISIS accelerator control room, where the magnetic induction must be less than 0.0005 T, from the MICE magnets. The stray field at the iron wall depends on the operating mode of the magnets. MICE may be operated in the pure flip mode (where the two coils in all of the AFC modules operate at the same current and at opposite polarity), or they may be operated in the pure non-flip mode (where both AFC coils operate at the same current and the same polarity). Note the other coils in MICE that are next to an AFC module operate at a polarity that is the same as the nearest AFC module coil. When MICE in stage-6 is operated wholly in the flip mode, the magnetic moment of the MICE channel is zero and the stray field at the iron wall is minimized. When the MICE cooling channel operates wholly in the non-flip mode, the magnetic moment generated by the cooling channel magnets is maximized. In this case, the stray field at the iron wall is also a maximum. There are operating cases where some AFC magnets operate in the flip mode and others operate in the non-flip mode. The stray field is in between the two extremes. The shield on the wall between the MICE hall and the ISIS control room is designed for the worst-case, where the muon momentum is 240 MeV/c and all three of the AFC magnets are run in the non-flip mode.

The fact that the magnets are not shielded means that field from a magnet can affect the magnets around it. As a result, there are forces between magnets [6], and there is coupling between the magnet coils and modules [7]. The cold mass support system design for each of the MICE magnet modules was set by the worst-case longitudinal magnet force on that module. The worst-case force occurs either during a quench or when the polarity of a magnet is accidentally reversed. The design criteria for the magnet cold mass supports were set based on the maximum magnet operating currents. This is when MICE is operating with muon beams at their highest design momentum of 240 MeV/c. The other consequence of having unshielded magnets is the magnetic field at the magnet coolers and at the top of the HTS leads. The effects of magnetic field are particularly important for the magnets in the RFCC module and the AFC module [8].

2. Cooling the MICE Magnets with Pulse Tube Coolers

The MICE magnets will be cooled using small coolers, even though the magnets and absorbers in a long muon-cooling channel would be cooled using a large refrigerator. The reason for using small coolers was cost of purchasing and installing a large helium refrigerator [9] at the Rutherford Appleton Laboratory (RAL), where the experiment is located. Studies of the use of small coolers for cooling the MICE magnets and liquid hydrogen absorbers were undertaken in 2004 [10], [11]. These studies resulted in the decision to cool the MICE magnets and absorbers using small coolers.

After some study, the decision was made to use Cryomech PT415 1.5 W (at 4.2 K) two-stage pulse tube coolers [12] [13] instead of the more standard 1.5 W GM two-stage coolers often used for MRI magnets. The primary reason for using pulse tube coolers was the fact that the coolers would be subjected to the stray magnetic field from the MICE cooling channel magnets [14]. The only part of a pulse tube cooler that is affected by the magnetic field is the rotary valve motor, which can easily be shielded for local magnetic fields of 0.25 T. Pulse tube coolers have the additional advantages of low vibration accelerations and a maintenance interval of 25000 hrs for the cold head rotary valve. (There are a number of Cryomech pulse tube machines that have run continuously over six years without cold head maintenance.) The primary disadvantage of using pulse tube coolers is the fact that the pulse tubes must be vertical with the cold heads of both stages in the down position. A PT415 cooler that is designed to be dropped into a cooler sleeve is shown in Figure 2.

The heat loads on the first stages of the coolers can be high, because of the heat coming from room temperature down the copper leads that are attached to the top of the HTS leads. (For an optimum pair of leads, this heat load is ~94 W per 1000 A lead pair at design current [15], [16].) Additional cooling for the leads could be provided using liquid nitrogen or additional single stage coolers. When the magnetic field is low locally, a large GM single stage cooler producing (up to 250 W at 55 K) can be used [17]. There is one single stage pulse tube cooler, which can operate in a magnetic field up to 0.25 T that is made by Cryomech. This cooler produces 60 W at 77 K [17].

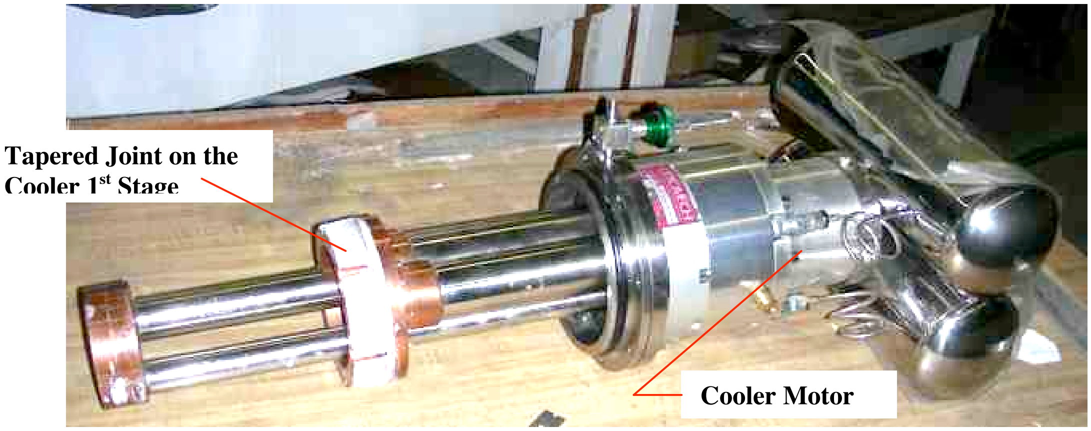

Figure 2. The Cryomech PT415 cooler (To the left is the cooler second stage with its condenser. The white part is the tapered drop-in part of the cooler first stage. To the right are the cooler rotary valve, the valve motor and the ballast tanks for the two cooler stages.)

The connection between the copper ring on the outside can containing the cooler and the first stage of the cooler is made through the tapered joint shown in Figure 2. The joint is designed to minimize the temperature drop between the outer copper ring and the first stage of the cooler. The tapered surface must carry the heat coming down the copper leads that connect to the HTS lead (theoretically the largest source of heat into the cooler first stage), the heat coming down to the cold mass supports to their thermal intercepts, heat conduction through tubes and wires, and the heat from 300 K that goes through the multi-layer insulation (MLI) and any holes that are in the MLI that can carry radiation from 300 K to the shield.

For the spectrometer solenoids and the coupling magnets, the coolers will be installed as drop-in coolers. This allows the cooler to be removed while the magnets are being shipped. The spectrometer solenoids will be shipped to Fermilab for magnetic measurement before they are shipped to RAL in the United Kingdom. The coupling magnets will be shipped from China to the Berkeley for final assembly with the RFCC cavity vacuum vessel before the RFCC components are shipped to RAL for assembly in MICE. Using the drop-in cooler mode permits one to ship the coolers separately thus avoiding damage to the coolers. The problem with using coolers in the drop-in mode is the thermal connection between the tops of the HTS leads to the first stage of the coolers.

The key to connecting the cooler cold head with the heat load immersed in a cryogenic fluid is creating a condenser circuit that causes the cryogen that cools the load to circulate. Simply immersing the cold head of the cooler into a bath of liquid cryogen does not work if one wants a low temperature drop between the source of the heat and the cold head. The re-condensing gravity thermal siphon circuit shown in Figure 3 will have a much lower temperature drop between the magnet cold mass exposed to liquid helium and the cooler cold head than any other method of connecting the cold head to the magnet being cooled [10], [18], [19]. Excellent vibration isolation can be achieved because the distance from the load to the cold head can be increased and the elements connecting the two can be flexible within the pressure constraints of the cooling circuit.

If one wants to have a low temperature drop between the magnet being cooled and the cooler 2nd stage cold head, the area of the cold mass exposed to liquid helium must be such that the heat transfer per unit area must be less than 2 Wm^{-2}. The area of the condenser must be large enough such that the heat flow per unit of vertical area must be less than 40 Wm^{-2}. Figure 4 shows the condenser that is part of the PT415 cooler second stage being used by LBNL for the spectrometer solenoids and the coupling solenoids. The condenser shown in Figure 4 has a vertical area of 0.042 m^2. In addition to the vertical area, the whole bottom of the second stage is also available for condensation.

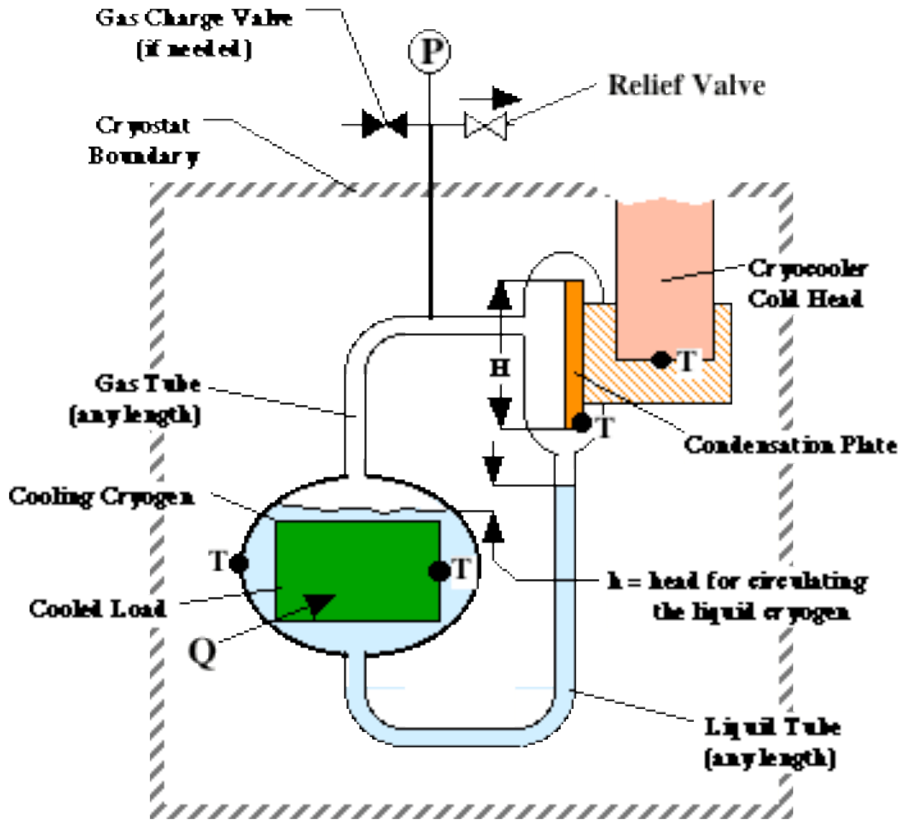

Figure 3. A schematic representation of a gravity thermal siphon connection between the cooler 2nd-stage cold head and the magnet cold mass (See [19]).

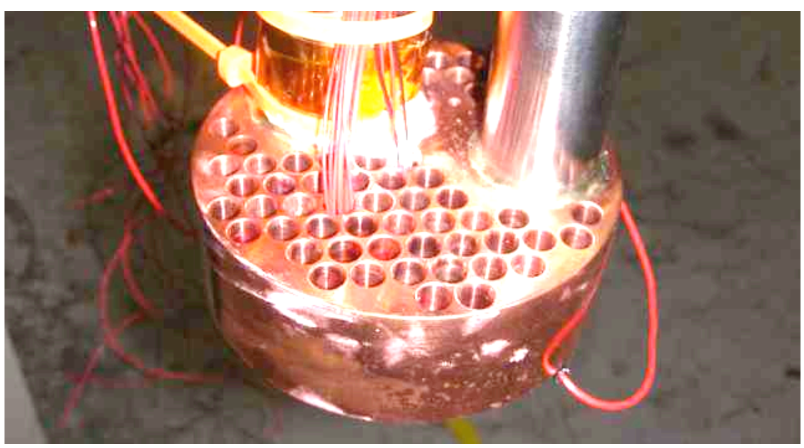

Figure 4. The second stage condenser of the PT415 coolers used for the spectrometer solenoid.

The Lawrence Berkeley Laboratory tested four drop-in coolers in a test facility at a magnet vendor's plant [20], [21]. Three cooler drop-in configurations were tested within the facility. Figure 5 shows the three configurations used in the drop in cooler test. Configurations A and B feed condensed liquid to the bottom of the cryostat. The boil off gas is fed to the condenser above the cooler second stage in configuration A. Configuration C is one that is often used for MRI magnets. Liquid drips off of the condenser; the gas goes along the condenser tube wall back to the condenser.

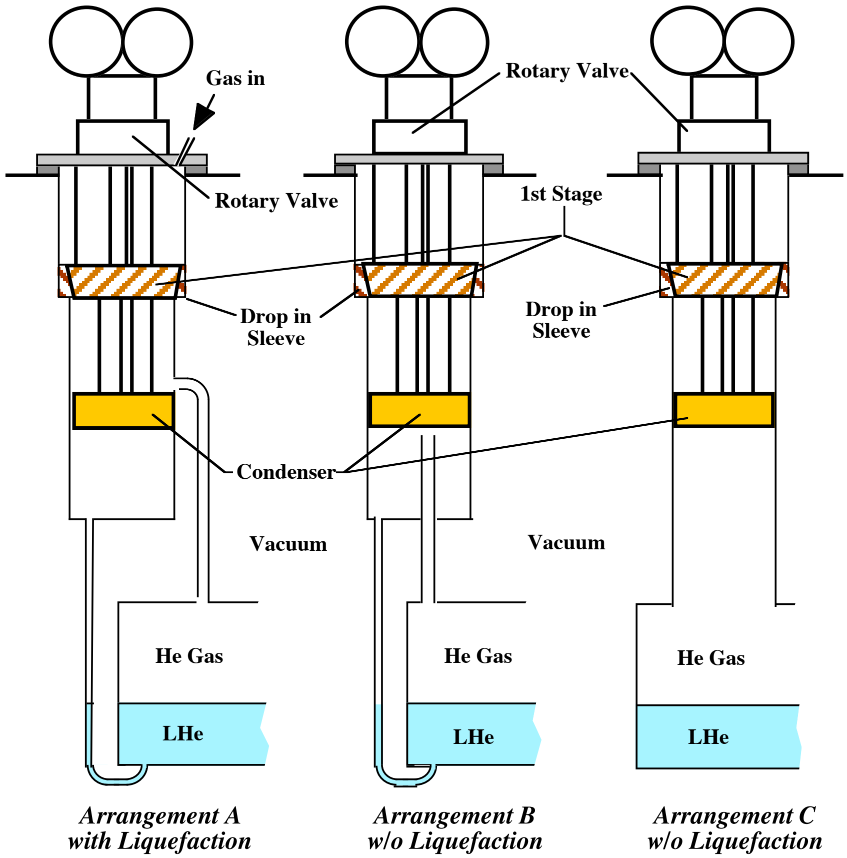

Figure 5. The configurations of the three drop-in cooler tests done by LBNL.

The three cooler test configurations are shown in Figure 5. Configuration B is the same as configuration A except that the boil off gas from tank is fed at the bottom of the condenser. Configuration B did not allow 300 K helium gas to be fed at the top of the cooler. All of the configurations produced re-condensation when up to 1.3 W of heat was applied on the bottom of the helium tank operating at a pressure of 1.013 bars. All three configuration produced re-condensation even when 40 to 55 W was applied to the sleeve that the cooler first stage drops into. The measured temperature drop with 50 W applied to the sleeve was ~3 K when the tapered copper first stage was in contact with the copper sleeve by itself. When a high conductivity grease is used between the first stage and the sleeve in the first stage joint, the temperature drop was reduced to ~0.5 K with the same 50 W being applied to the sleeve. The first stage temperature is ~54 K with 50 W applied.

Configuration A cooled down the cooler second stage, the condenser, the sleeve around the condenser, and the helium tank from 300 K to 4 K. When 300 K helium gas entered the cooler space above the first stage, helium was liquefied into the tank. Despite the fact that there was no extended heat exchanger connected to the cooler first stage, helium liquefaction up to 0.01 g s^{-1} occurred. Configurations B and C cannot liquefy helium. The cool-down rate for configuration C is much slower than for configuration A. All configurations worked fine for helium re-condensation as long there is liquid helium in the tank. The problem with configurations A and B, is the trap that is formed by the pipe that connects the bottom of the condenser sleeve with the bottom of the liquid helium tank. This trap can become clogged with dirt, frozen water and frozen air gasses. A small amount of dirt or ice is not much an issue when configuration C is used.

3. Progress on the MICE Spectrometer Solenoids

The work on the MICE spectrometer solenoids was started in 2003 at INFN Genoa. A design emerged that was compatible with the MICE lattice [22]. The design that evolved had two match coils (to match the beam with the focusing magnets) and a three-coil spectrometer solenoid that was designed to produce a uniform magnetic field (better that 0.3 percent) within a volume that is 1-m long and is 0.30 m in diameter [23]. The magnet design evolved when INFN was forced to abandon the project in 2006 due to funding difficulties. The Lawrence Berkeley Laboratory took over the design and fabrication of the spectrometer solenoid at that time. A design evolved that was similar to the INFN design except that the magnet conductor was the same as that proposed for the focusing and coupling magnets. As a result of a lower copper to superconductor ratio, the coil current density increased while maintaining the same temperature margin as the INFN magnet design [24] [25].

The cold mass mandrel was fabricated from a single forging made from 6061-T6 aluminum. The forging was machined to accommodate the coils, the quench protection diodes and about 190 liters of liquid helium. A three-dimensional schematic view to the spectrometer magnet cold mass is shown in Figure 6. The finished cold mass assembly is 2511 mm long. The five coils are clearly shown in Figure 6. The coils at the AFC end of the magnet M1 and M2 tune the muon beam coming from the focusing magnet to the three-coil spectrometer magnet (End1, Center, and End 2). End coil 1 can also play a minor role in the muon beam tuning process.

The conductor that was ordered was similar to conductor used for an RF cavity test solenoid built for Fermilab in 1998 [26]. We expected to order a Nb-Ti conductor with about 55 filaments that were 80 μm in diameter. We instead received a conductor with 222 Nb-Ti filaments that are 41 μm in diameter. The conductor copper to superconductor ratio is 4; the RRR of the copper is about 70; and the conductor twist pitch is 19 mm. The conductor was insulated with a layer of Formvar 25 μm thick. The insulated dimensions of the coil superconductor are 1.00 mm by 1.65 mm, which is identical to the conductor used in the Fermilab solenoid. Four billets of this conductor were delivered in six pieces from 5-km long to 33-km long. The conductor cross-section is shown in Figure 7.

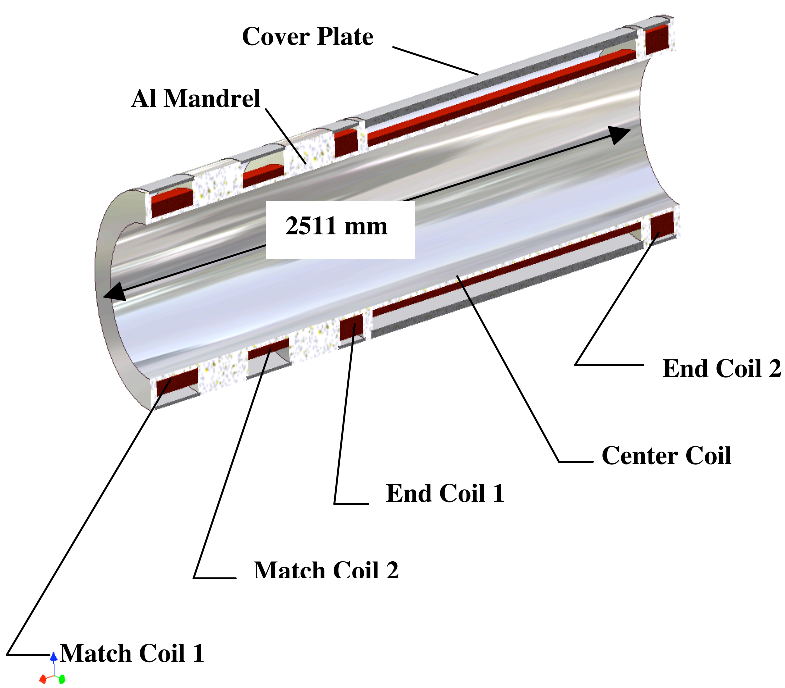

Figure 6. A three-dimensional schematic view of the spectrometer solenoid cold mass.

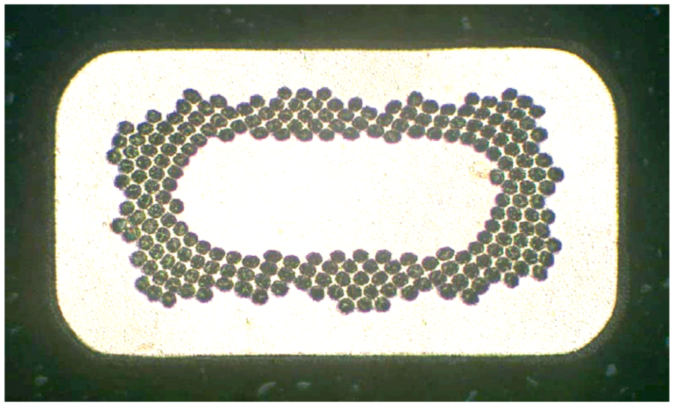

Figure 7. The conductor cross-section for the spectrometer solenoid conductor.

The winding of the first spectrometer solenoid began in the spring of 2007 (See Figure 8). The first cold mass assembly was completed in the in the late fall of 2007 (See Figure 9). The self-centering tension band cold mass supports were assembled and tested. The cold mass supports are designed for 500 KN along the magnet axis. Assembly of the first magnet into its cryostat vacuum vessel was done during early 2008 [27]. The completed assembly of the first magnet was finished in the late spring of 2008 (see Figure 10). The first coil test was done during the summer of 2008 [28].

Figure 8. The winding of spectrometer magnet one (summer 2007).

Figure 9. The completed magnet one cold mass assembly (fall 2007).

Figure 10. The finished first spectrometer solenoid during the magnet test (July 2008).

The first cool-down of magnet one started in June 2008. The magnet cooling to 80 K used liquid nitrogen. The cool-down rate was controlled so that the cold mass cover plate welds would not be over stressed. The cool-down from 80 K to 4 K was done using liquid helium. The three pulse tube coolers were started after the magnet reached 20 K. The coolers were used to cool the magnet shield and the cold mass intercepts. The magnet design called for a shield temperature of 70 K. The cold mass support intercepts were not supposed to be above 80 K. The shield took a long time to cool-down. It never got down its design temperature. The center of the shield reached ~93 K while the ends reached ~108 K. The temperature of the copper plates, outside of the coolers, reached temperatures from 55 K to 62 K. The temperature on the copper plate on the top of the HTS leads furthest from the cooler reached about 61 K (with no current in the leads). While the shield temperature was abnormally high, the temperature at the top of the HTS leads seemed correct.

Once the magnet was filled with liquid helium, it was trained to 196 A (~70 percent of its design current) in a couple of quenches. The passive quench protection that employs quench back and cold diodes worked well [29]. The quench testing was stopped, because the coolers were not holding the heat load. In fact, the helium boil off was 6 to 8 liters per hour, which meant that an excess heat load of 3.7 W to 5.1 W was entering the cold mass. The temperature on the outside of the can around the condenser seemed to be quite low, especially late in the test. This is an indication that the three coolers were producing very little 2nd stage cooling. There was either a problem with the coolers or there was a problem with the flow circuits that carried the cooling to the cold mass [28].

The circuit that carried liquid helium from the condenser to the bottom of the cold mass helium vessel looked a lot like arrangements A and B in Figure 5. When the magnet was warmed up above 80 K, it became clear that the pipes that went from the cooler condenser can to the bottom of the cold mass helium tank were plugged with nitrogen ice. Liquid nitrogen present in this tube during the magnet cool-down remained within the tube trap at the bottom of the helium tank (see Figure 5B), as the tank was being pumped and purged before liquid helium cooling. A second problem was that the thermal connection the between the cooler first stage and the 6061-T6 aluminum shield was not adequate. This was blamed on the copper straps between the cooler sleeve shield and the magnet shield. A third issue was the desire to pre-cool the aluminum shield before the coolers are turned on. We made changes on both magnets in order to address the three issues given above.

The winding of the second magnet started in the in the summer of 2007. Because the first magnet was being assembled, the second cold mass assembly was not completed until the summer of 2008. The needed changes indicated by the first coil test were made. A liquid nitrogen tank was attached to the large 6061-T6 shield, so that the shield could be pre-cooled. Arrangement C was adopted for re-condensation in the spectrometer solenoids. The copper connecting straps were replaced with large flexible 1100-O aluminum straps that would have several times the conductivity of the previous copper straps. Despite this change, the thermal connection to shield was still poor. The method of surveying the magnet into the cryostat vacuum vessel was greatly improved. When the second magnet cold mass was installed, its position was known to about ±200 μm compared to fiducials on the outside of the cryostat. Table 1 shows the as built parameters of the second spectrometer magnet.

Table I. The As Built Parameters for the Second Spectrometer Solenoid

Parameter	Match 1	Match 2	End 1	Center	End 2
Inner Coil Radius (mm)	258	258	258	258	258
Coil Thickness (mm)	46.165	30.925	60.905	22.125	67.783
Coil Length (mm)	201.268	199.492	110.642	1314.30	110.642
Current Center Axial Position* (mm)	124.00	564.00	964.00	1714.00	2464.00
Current Center Radial Position* (mm)	281.083	273.463	288.453	269.063	291.891
Coil Average J (A mm^{-2})	137.67	147.77	124.28	147.66	127.09
Number of layers per Coil	42	28	56	20	62
Number of Turns per Layer	115	114	64	768	64
Total Number of Turns	4830	3192	3584	15360	3968
Design Current (A)**	264.83	285.60	233.68	275.52	240.21
Coil Self Inductance (H)^	12.0	5.0	9.0	40.0	11.3
Coil Stored Energy (MJ)**	0.42	0.20	0.26	1.55	0.32
Peak Field in Coil (T)**	5.30	4.32	5.68	4.24	5.86
Temperature Margin at 4.2 K (K)**	~1.6	~1.8	~1.5	~2.0	~1.5

* Based on Z = 0 is at the match coil end of the magnet cold mass. (The center of MICE in these coordinates is at Z = -3487 mm.) R = 0 is the axis of the magnet (the MICE axis).

** This is at the maximum design current, which is based on the worst-case currents for the five coils.

^ The inductance of the two end coils and the center coil in series is about 74 H.

There are differences between magnets one and two [30]. The axial position of the current centers for the two magnets is the same within ±20 μm. There are variations in the radial position of the coil current centers by as much as 370 μm. This difference is of little concern because the integrated field is the same for both magnet coils. The number of turns in both magnets is the same for the two match coils, End 1 and End 2. The center coil for magnet two has eight more turns than the center coil of magnet one. This is equivalent to a current change between the two coils of 0.15 A (about 0.051 percent). It was felt that this is of little concern. A current correction can be made in the center coil.

Magnet two was tested in June and July of 2009. The magnet was powered to 238 A (~87 percent of design current) with all five coils in series. The current test was stopped because the one of the HTS leads burned out. The shield was ~10 K warmer than for the first magnet. At the same time, nitrogen in the tank was being boiled at the rate of 0.75 L hr^{-1} (an added 31 W). The temperature near the cooler first-stages varied from 66 K to 74 K. The temperature at the far end of the leads was 81 K, even with no current in the leads. The lead that burned out was at the end farthest from the coolers. If one looks at the characteristics of the HTS-110 leads used in the magnet, the lead should have burned out at a current >200 A. The heat leaks into the magnet shield and leads appeared to be excessive.

The spectrometer solenoid for MICE is one of the largest magnets that has been cooled using small coolers. When one combines the physical size of the magnet (2.7 m long by 1.4 m in diameter not including the service tower for the coolers, leads and LN_2 tank) with a large cold mass (>4 metric tons) and nearly 1000 A of conduction cooled lead pairs, one can see why it is difficult to keep the magnet cold using three PT415 coolers alone. A single stage GM cooler will be used to provide the extra cooling (up to 185 W at 55 K) that may be needed for the magnet shields and HTS leads. Fortunately, the magnetic induction is low (< 0.05 T) where the GM cooler is to be located.

Despite, a high shield and intercept temperature (too high by 30 K) and a higher temperature at the cooler first stages (from 12 to 18 K), the cooler second stages behaved well. At a helium pressure of 1.1 bars, the helium boil off rate was 0.125 L hr^{-1}. (The heat leak is too high by ~0.09 W.) It is believed that if the shield and cooler first stage temperatures can be brought down, the three PT415 coolers can provide enough refrigeration to keep the second spectrometer magnet cold at full current.

The power supplies and the magnet rapid discharge system were tested. The behavior of the power supplies and their controllers was not fully understood. A rapid discharge varistor (diode) system was built to allow the spectrometer magnets to be discharged in the event of a power failure that would put the coolers out of commission [31], [32]. This would allow the magnet to be discharged fast enough to keep the HTS leads from burning out. When the two match coils in series were discharged through the rapid discharge system, the discharge occurred without a problem. When a single match coil was discharged through the system, the magnet quenched. This was probably caused by excessive voltages across the quench protection diode for the match coil. More study is needed.

It is hoped that information gained from the fabrication and testing of the spectrometer magnets can be applied to the other magnets in MICE. A key lesson learned is the importance of controlling the heat flow to the first-stage of the coolers. PT415 coolers work best when the first-stage is <55 K.

4. Progress on the MICE Coupling Solenoids

The work on the MICE coupling solenoids was started in 2003 at Oxford University. The design that emerged in 2004 was compatible with the MICE lattice [21]. The design that evolved was a single short superconducting magnet. The magnet cryostat length was limited by the space between the RF cavity couplers [33]. A study was undertaken concerning the use of a much longer coupling coil [34]. The study found there was a real benefit in lengthening the magnet. This concept was rejected because each 201.25 MHz RF cavity had to be individually powered through its own coupler. The meant that the coil had to split with room temperature holes between coils. The position of the coupling coil around the rest of the RFCC module is shown in Figure 11. (The coolers are not shown in Figure 11.)

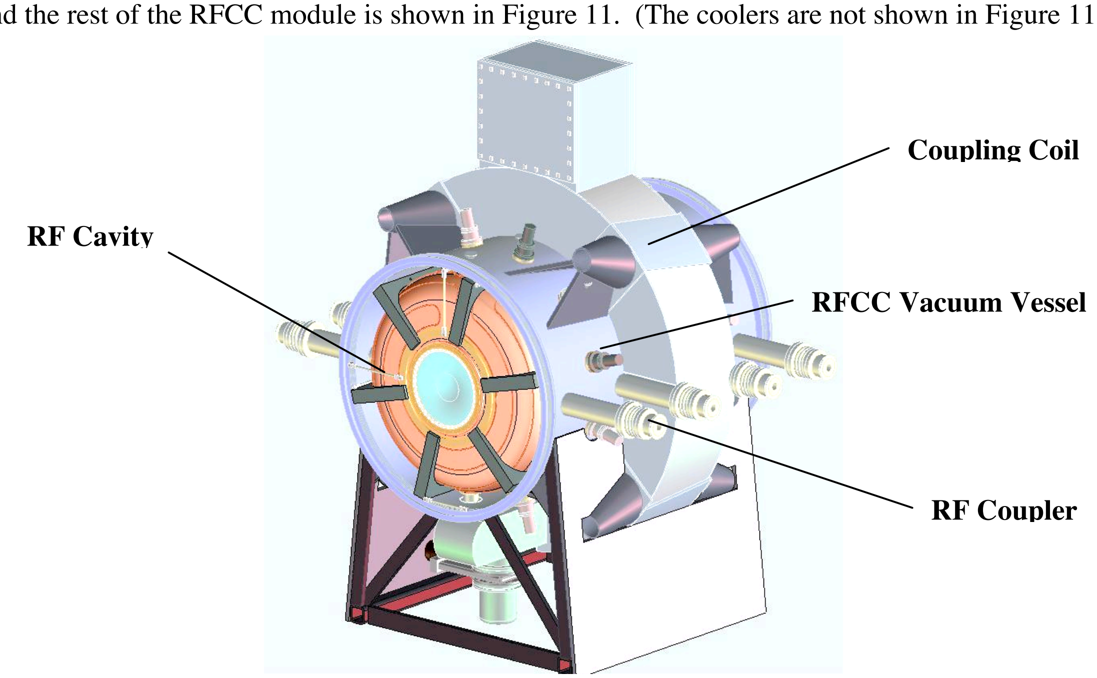

Figure 11. The RFCC module with the RF Cavities, the RF couplers and the coupling magnet.

From Figure 11, it is clear that the inside diameter of the coupling coil cryostat is set by the outside diameter of the RFCC vacuum vessel that contains the RF cavities. Thus the inner coil radius was set to 750 mm. Once the inner diameter of the coil is set, the other radial dimensions build out from that.

The Institute of Cryogenics and Superconductivity Technology (ICST) at the Harbin Institute of Technology (HIT) formally joined the MICE collaboration in 2006. ICST started an engineering design of the coupling magnet in early 2007. The coupling coil length was increased to 285 mm. As result, the peak field in the winding decreased from 7.7 T to 7.4 T, which resulted in a larger temperature margin. The cryostat vacuum vessel was designed to fit around the RF cavity couplers.

The magnet coil will be wound on a 6061 aluminum mandrel. The first issue that was dealt with was whether the magnet could be cooled using liquid helium in a tank outside of the magnet coil. Since a magnet helium vessel must be designed in accordance with the pressure vessel code, the stress due to cool down and magnetic forces had to be added to the stress due to the helium pressure. As result, the magnet will be indirectly cooled using liquid helium in tubes imbedded within the cryostat cover plate. The magnet structure isn't subject to the pressure vessel code. Figure 12 shows a three-dimensional view of the latest design of the MICE and MuCOOL coupling coils [35] [36].

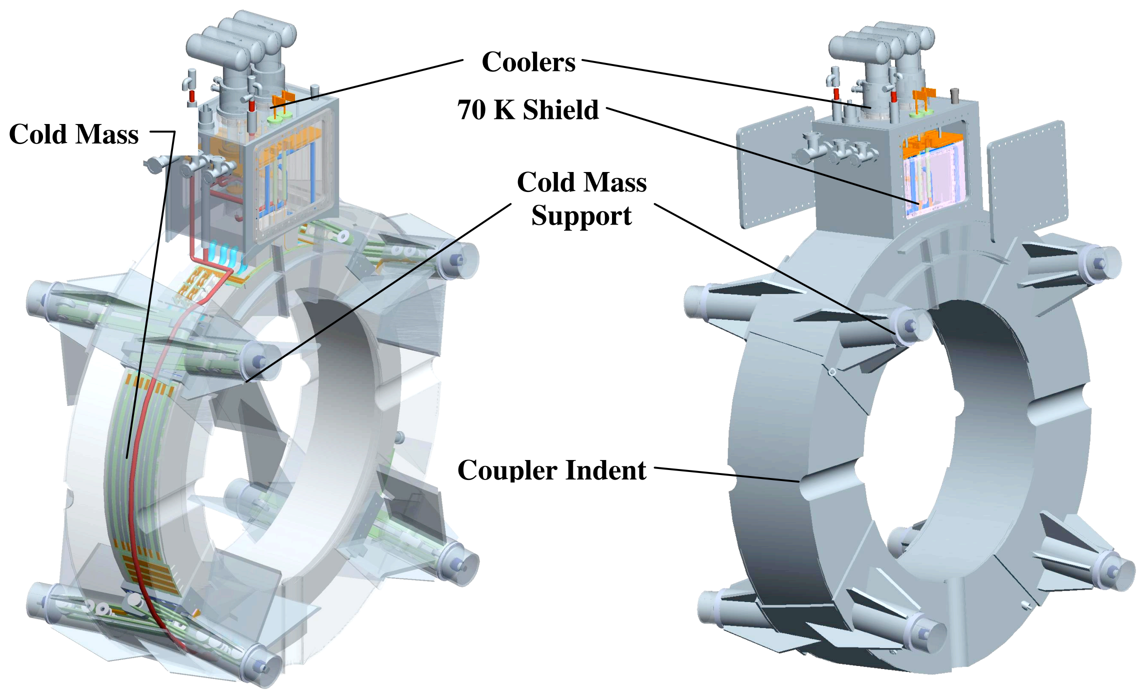

Figure 12. A three-dimensional view of the MICE coupling magnet. (The figure on the left shows the magnet within its cryostat. The figure on the right shows the coupling coil cryostat.)

The coupling magnet will be wound with the conductor in tension at a stress of ~60 MPa. After the coil is wound, it will be banded with a material not yet selected [35]. The coil is in compression radial direction. As a result, the boundary between the coil and the mandrel is never in tension even when the magnet is fully charged. Cooling tubes will be welded in the cover plate. These tubes will connect the tanks at the top and bottom of the coil. The tube that carries liquid from the top tank to the bottom tank must be insulated from the cold mass. A gravity fed thermal siphon circuit will keep the cold mass cold. The top tank is connected to the cooler using arrangement C in Figure 5.

Table 2 shows the basic parameters for the coupling magnet. Figure 13 shows a 3-dimensional cross-section view of the cold mass, showing the mandrel, the coil, the banding, the cover plate and the tubes that carry helium from the bottom tank to the top tank. Figure 14 shows one pair cold mass supports (one of four pairs) for the coupling magnet [37]. The supports are roughly 90 degrees apart.

Table 2 Basic Coupling Magnet Parameters

Parameter	Flip	Non-flip
Coil Length (mm)	285	
Coil Inner Radius (mm)	750	
Coil Thickness (mm)	102.5	
Number of Layers	96	
No. Turns per Layer	166	
Self Inductance (H)*	591.8	
Magnet J (A mm^{-2})*	114.6	108.1
Magnet Current (A)*	210.1	198.2
Stored Energy (MJ)*	13.1	11.6
Peak Induction in Coil (T)*	~7.4	~7.0
Temperature Margin (K)*	~0.8	~1.1

* Worst Case Current when p =240 MeV/c, β = 420 mm

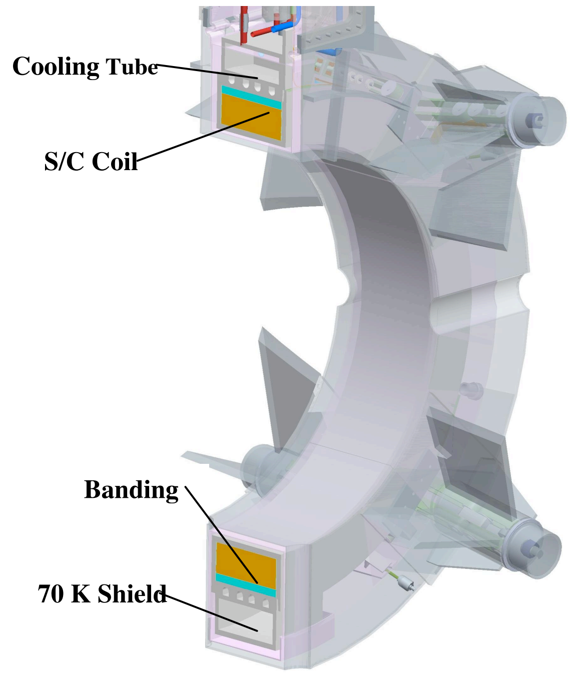

Figure 13. Coil cold mass structure.

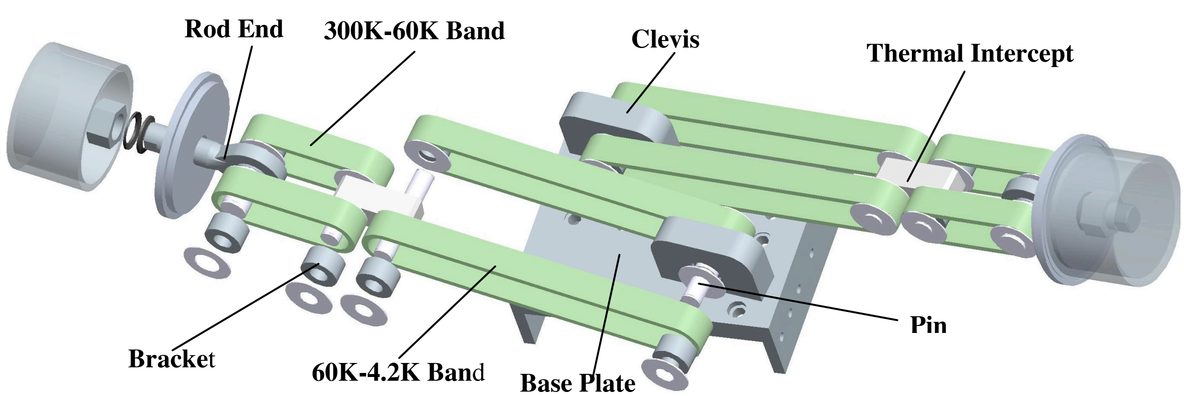

Figure 14. The double-band cold mass support assembly for one of four coil positions.

The support assembly shown in Figure 14 is one of four such assemblies spaced 90 degrees apart. The stainless steel base plates with their clevises are bolted to the cold mass cover plate. The 150 kN pretension forces are carried by the stainless steel plate instead of the cold mass. The four cold mass assemblies are designed to carry 500 kN from 4 K to 300 K along the magnet axis. The support system will carry 50 kN in the radial direction. The support bands shown above are similar to the bands for the MICE spectrometer solenoid. A similar concept is planned for the MICE focusing coils. The cold mass forces are carried to the RFCC vacuum vessel through the gussets around the room temperature can at the warm end of the cold mass support.

The 70 K shield will be fabricated from 1100-0 aluminum, which has a larger thermal conductivity than 6061 aluminum. Two coolers produce ~110 W at 55 K (at the 1st-stage). This should be adequate to cool one pair of 210 A copper leads, the heat flowing to the cold mass intercepts and shield as well as piping and instrumentation wires. The multi-layer insulation can be spooled onto the cold mass as a single piece. This should reduce thermal radiation into the magnet cold mass.

In terms of the stray field generated by the MICE magnets, the coupling coil is the elephant in the room. A single coupling coil generates a magnetic moment of 2.15 MA m^2, which is three and a half times the magnetic moment generated by all coils in the spectrometer solenoid. The stay field is also high next to the magnet coils. Where the quench protection diodes are located the stray field will be from 1.5 T to 3.0 T. The stray field at the top of the HTS leads is about 0.3 T. It is important the HTS leads be oriented correctly and their temperature be kept below 60 K [38].

ICST fabricated two tests coils. The small test coil, with an ID of 350 mm and a length of 285 mm, was built to test the winding machine using the actual coupling magnet superconductor [38]. The coil will later be used to do tests of quench protection diodes at 4 K, 77 K and 300 K. These tests will be done in a magnetic field up to 4 T that is both parallel and perpendicular to the diode junctions. The cold diodes in the coupling coil will be in a magnetic field up to 3 T.

ICST has spent a considerable amount of time developing low resistance splices that can be wound into the coupling coils. The superconductor that has been purchased for the three coupling coils is identical to the conductor used for the spectrometer solenoids. The yield for this conductor used in the spectrometer solenoids was very good. This is not true for the coupling magnets. The three Chinese coupling coils (two coupling coils for MICE and one coil for MuCOOL at Fermilab) require eight billets of conductor. The same vendor that provided the spectrometer solenoid conductor eighteen months earlier ended up processing twelve billets of conductor to get forty pieces that ranged in length from 4 km to 12 km. We don't know why the yield was so bad on the second batch of conductor. As a result, the coupling coils will have a lot of splices in them. The maximum allowable resistance for the splice was set at 10 nΩ. A series of tests were run of splices made with two types of solder. One-meter long splices with resistances from 1 to 1.8 nΩ have been fabricated by ICST [39].

A large test coil, with an ID of 1500 mm, a length of 72 mm and a thickness of 103 mm (a quarter length coupling magnet), was built to strain the magnet conductor to the same strain that will be encountered in the coupling coil at full current [40]. The winding of the splices into a coil became part of the large coil-winding test. The winding of the large test coil at ICST is shown on the left side of Figure 15. The installation of the insulated large test into the large vacuum vessel that will be used to train the MuCOOL and MICE coupling coils is shown on the right side of Figure 15. The tubing shown on the right side of Figure 15 distributes liquid helium to the cooling circuit that is on the outside of both test coils. The current enters the magnet through 500 A gas-cooled leads.

Figure 15. The large ICST test coil. (Left, the large test coil is being wound on the ICST winding machine. Right, the insulated large test coil is being lowered into the large ICST vacuum chamber.)

Figure 16. The rough coupling coil mandrel as prepared for heat treatment before machining.

The large test coil was cooled down in April and May of 2009. The magnet got cold enough to become superconducting, but the magnet didn't get cold enough to run current into the magnet. The cooling system must be modified so that the full mass flow from the refrigerator J-T circuit can be used to keep the magnets cold. Using a refrigerator permits one to train the coupling coils to their full design current before they are installed in their final cryostat and connected to the coolers.

In early 2009, ICST contracted with the Qi Huan Company in Beijing to build the coupling magnets. This company has built a number of MRI magnets, and it is very good at welding of aluminum. The Qi Huan Company tested a number of weld samples for the coupling magnet. A number of these weld samples have been heat-treated and strength tested. The strength weld material in the mandrel can be improved from 140 MPa to 225 MPa with proper heat treatment. However, this heat treatment is difficult in something the size of the mandrel shown in Figure 16. (The flange diameter is ~1.8 meters. The height is about 335 mm.) The company has also fabricated the first magnet cover plate made from a forged plate of 6061-T6 aluminum. In the mean time, the company has been winding their own test coils, which are similar to the coils made by ICST. The quality of the coil winding and wet lay-up appear to be quite good. Conductor splices fabricated by Qi Huan were tested at LBL in September 2009. The Qi Huan splices are very good.

5. Progress of the MICE Focusing Modules

The AFC module is the smallest of the three MICE modules. It is also the most complicated module of the three modules. Magnetic field is combined with ionization cooling in the AFC module. There will be solid absorber or a liquid hydrogen absorber within the 470 mm warm bore of the magnet. The clearance between the OD of the liquid hydrogen absorber and the warm bore of the focusing solenoid is about 35 mm. Within this 35 mm radial space is plumbing for the absorber, MLI for the absorber, and cold mass supports that separate the absorber from the magnet bore, which is warm compared to the absorber [41]. Figure 17 shows the LH_2 absorber within the focusing magnet bore.

The length of the coil cold mass and the magnet cryostat vacuum vessel are limited by the module length and the fact that supply and return pipes must go up past the end of the coil cryostat in the hydrogen vacuum space (see Figure 17). The AFC module has two vacuum spaces, the cryostat vacuum for the superconducting magnet and the insulating vacuum around the liquid hydrogen absorber. The ends of the AFC modules share a common vacuum with either the spectrometer solenoid bore, or the vacuum that is around the RF cavities in the RFCC module.

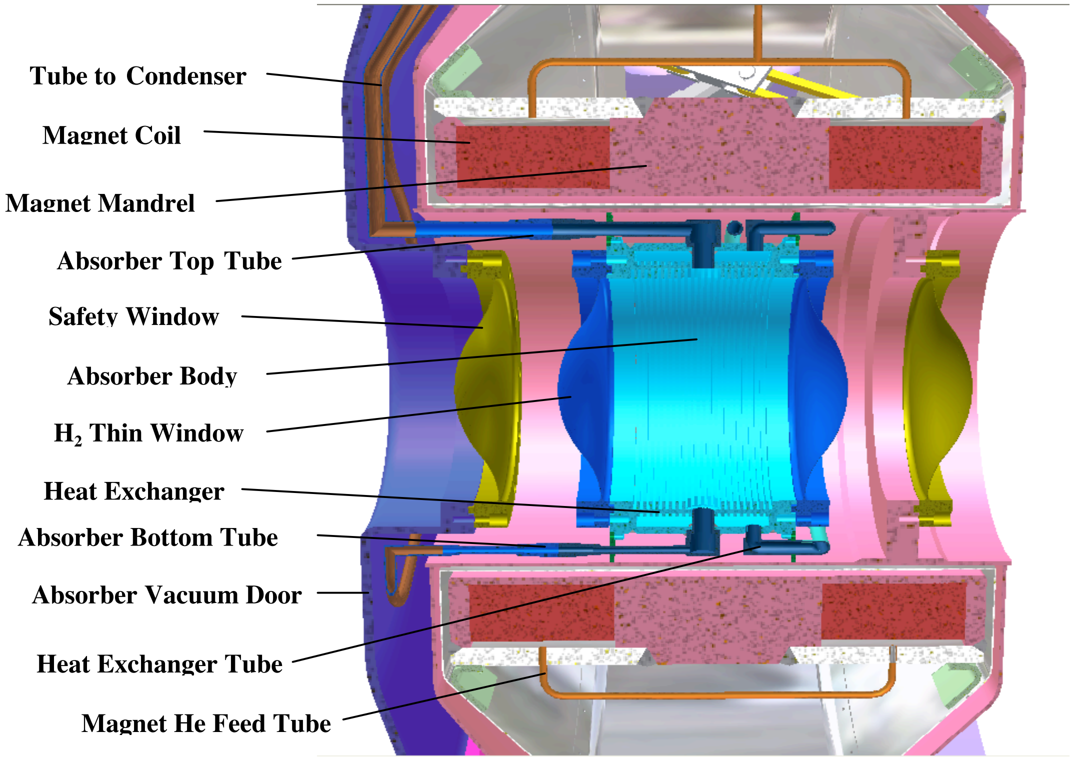

Figure 17. A three dimensional cross section of the MICE liquid absorber showing the absorber liquid volume, the absorber body, the body heat exchanger, the thin windows and the hydrogen feed tubes.

Design work on the focusing magnet module began in 2003. The magnet design was based on the RF cavity split solenoid that LBL had built for Fermilab. The coils in the MICE focusing magnet design that was started in 2003 were shorter and thicker than the coils actually built for the magnet finished in 1999 and tested later that year [26] [42]. The solenoid built for Fermilab had the coils closer together than the MICE focusing magnet. The axial distance between the current centers was 390 mm versus 410 mm that was arrived at for the MICE focusing magnet design. The inner coil bore of the MICE focusing magnet (526 mm) is nearly the same as the Fermilab split solenoid (520 mm). The Fermilab solenoid quenched at 253 A (110 percent of maximum design current) in non-flip mode. In the flip mode the Fermilab magnet was run up to 294 A, the limit of the power supply, without quenching [43]. Since the Fermilab magnet was nearly identical to the focusing magnet magnetically, it was felt that this was proof positive that the focusing magnet could be successful as designed.

Like the Fermilab split solenoid, the MICE split solenoid is designed to operate in the flip mode (the cusp mode with the polarity of the two coils in opposition) and the non-flip mode (the solenoid mode with the polarity the same for both coils) [44]. The Fermilab magnet was wound on a machined forged 6061-T6 mandrel. The mandrel caused quench-back into the magnet, which speeded up the quench process [45]. Since the Fermilab magnet quenched at stored energies similar to the design stored energies for the focusing magnet (in both modes), it was felt the passive quench protection system would work well.

Each coil in the Fermilab magnet had its own leads that went to room temperature, which permitted one to operate the magnet in the two modes. The MICE focusing magnet will have separate leads for each coil for the same reason. The Fermilab magnet has external (warm) quench protection diodes and resistors to reduce the voltage to ground within the magnet. The MICE focusing magnet will have cold diodes and resistors that do the same thing.

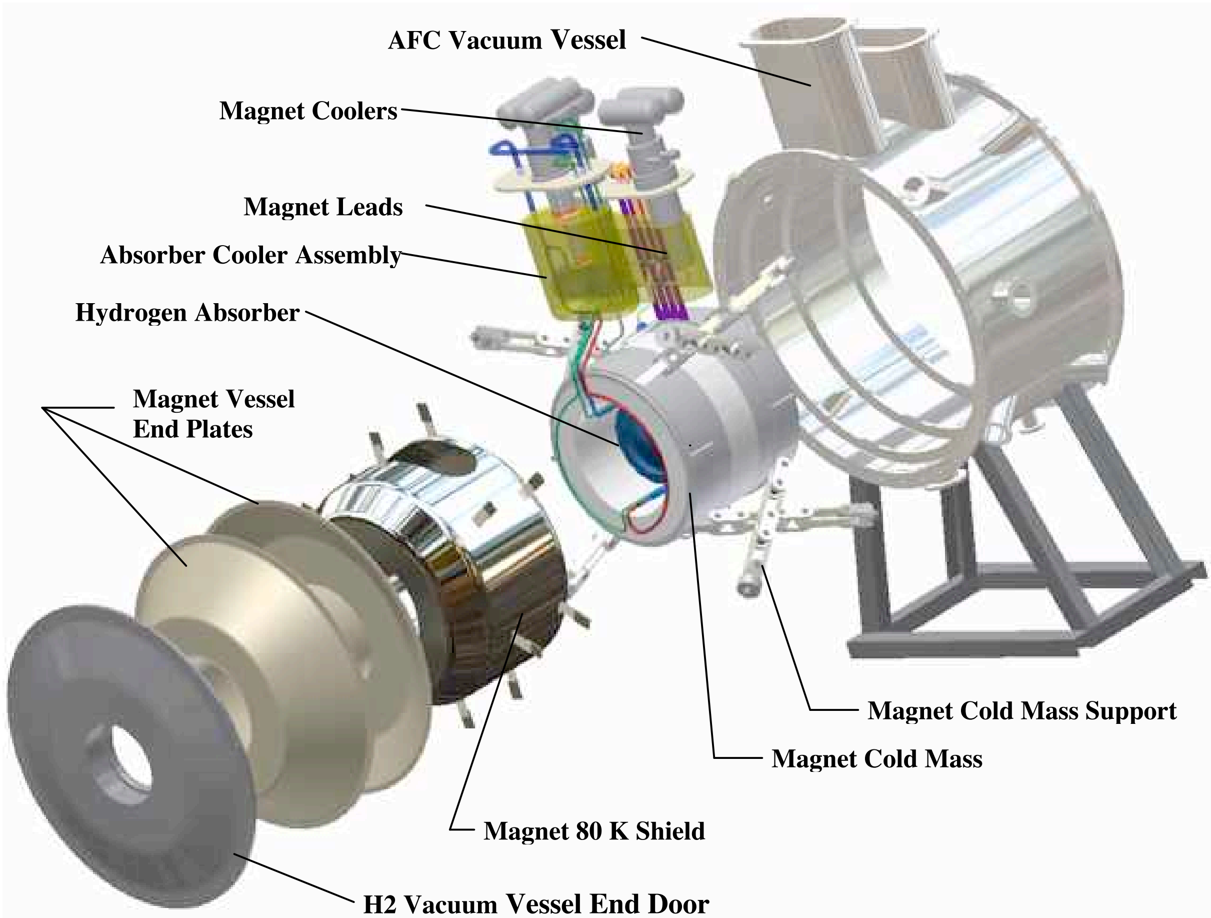

Figure 18. A schematic exploded view of the AFC module showing the magnet and the absorber.

Figure 18 shows a schematic of the AFC Module. The magnet cold mass is the central element of the module assembly. The magnet cryostat vacuum vessel consists of two end plates and a warm bore tube that is welded to the AFC module vacuum, vessel. Between the magnet cold mass assembly and the magnet vacuum vessel is a shield that will nominally be between 70 and 80 K. This shield is cooled by the first stage of the two PT415 coolers that keep the magnet cold. A single band cold mass support system is shown schematically [46], but the final design for the cold mass support bands may be different. The cold mass supports are designed for a maximum axial force (along the magnet axis) of 900 kN. The design radial force for the cold mass support system is greater than 50 kN.

The liquid hydrogen system for the absorber will be kept cold using a single PT415 cooler [11]. This cooler should be able to liquefy the hydrogen into the absorber. An alternative to using a cooler to liquefy the hydrogen is to cool the absorber heat exchanger with liquid helium while liquefying the hydrogen into the absorber. The first stage of the absorber cooler is used to cool the shield around the condenser tank that can store extra liquid hydrogen for the absorber when the absorber is above 21 K.

The magnet will be kept cold using two PT415 coolers. The critical issue is the first stage temperature and the temperature of the upper ends of the four HTS leads. There are four copper leads that connect to the upper end of the HTS leads. These copper leads are nominally designed for 250 A. Heat leak from the copper leads alone is expected to be about 24 watts per cooler. In addition each cooler will remove half the magnet shield heat load, half the cold mass support intercept heat load, and half the heat flow coming into the cryostat from piping and instrumentation wires.

Table 3 Nominal Focusing Magnet Operating Parameter in the Flip and Non-flip Modes

Parameter	Non-Flip	Flip
Warm Bore Radius (mm)	235	
Outer Cryostat Radius (mm)	700	
AFC Module Length (mm)	844	
Magnet cryostat Length (mm)	745	
Magnet Cold Mass Length (mm)	690	
Coil Inner Radius (mm)	263	
Coil Thickness (mm)	84	
Number of Coil Layers	76	
Number of Turns per Layer	127	
Magnet J (A m^{-2})	72.0	138.2
Magnet Current (A)	130.5	250.7
Magnet Self Inductance (H)	137.4	98.6
Peak Induction in the Coil (T)	5.04	7.67
Magnet Stored Energy (MJ)	1.17	3.10
Magnet 4.2 K Temp Margin (K)	~2.0	~0.8
Induction at R = 0.7 m (T)	0.12	0.66
Field Line Direction	Axial	Radial
Magnet Inter-coil Force (MN)	-0.56	3.53

* Currents at p = 240 MeV/c and β = 420 mm

Table 3 presents the nominal operating parameters for the focusing magnet. Many of the values given in Table 3 were in the specification that went to the bidders during the procurement process. Tesla Ltd in the United Kingdom was the successful bidder. Engineering on the magnet started in late 2007. Many of the values given in Table 3 come from Tesla Ltd. The length of the cold mass and the length of the magnet cryostat are different from the original design set forth in 2004. The cold mass length was increased from 670 mm to 690 mm. The end flange was thickened by 10 mm at both ends of the coil package. As a result, the cryostat length was increased from 725 mm to 745 mm. There will be changes to the parameters in Table 3 once the vendor starts winding the coil.

The superconductor the vendor bought is slightly different from the conductor used in the spectrometer and coupling solenoids. The bare focusing magnet conductor is 0.95 mm by 1.52 mm, which means that the conductor is slightly smaller than the conductor that was used to develop the design that is shown in Table 3. The focusing magnet conductor has a copper to superconductor ratio of 4. The filament diameter in the focusing magnet conductor is about 40 μm. The twist pitch of the focusing magnet conductor is nominally the same as the spectrometer and coupling magnet conductor.

The vendor will use vacuum impregnation to pot the focusing coil rather than a wet lay-up that is being used in the other two MICE magnets. This may result in a coil that has inter-layer insulation that is thicker than the 110 μm inter-layer insulation shown in Table 3. This could change the number of layers in the coil. Since the focusing magnet conductor is not as wide as the conductor used in the spectrometer and coupling magnets, the number of turns per layer may be different than is given in Table 3. The total number of turns in the coil is not expected to be grossly different from the 9652 turns per coil that is given in Table 3

Figure 19. A rough machined focusing magnet mandrel (left) and a forged cover plate (right).

Rough machining of the first mandrel has been done at the vendor. The forged mandrel cover plates have also been fabricated. The rough machined mandrel is shown on the left side of Figure 19. A rough forged cover plate for one end of the mandrel is shown on the right side of Figure 19.

The magnetic moment for the focusing magnets is the lowest of the three types of cooling channel magnets. In the flip mode, the net magnetic moment for the magnet is zero. In the non-flip mode at the nominal p = 240 MeV/c, β = 420 mm (at a current of 130 A), the net magnetic moment for the focusing magnet will be 0.23 MA m^2. Thus the stray field from the coupling magnets far away is quite low. The stay field far from the magnet in the flip mode is lower than the stray field far from the magnet in the non-flip mode.

The magnitude of the stray field close to the magnet coils is another matter. In the non-flip mode, the field at the vacuum vessel surface (R = 700 mm with 130 A in the coils) is 0.12 T. In general, the field is in the axial direction. In the flip mode, the field at the vacuum vessel surface (R = 700 mm with 250 A in the coils) is 0.66 T with a strong radial component. In the flip mode, magnetic field will affect both the HTS leads and the PT415 cooler rotating valve motors [8], [14], [38]. The position of the coolers and the HTS leads in the focusing magnet will be determined by the stray field in the flip mode at p =240 MeV/c and β = 420 mm (the worst-case). Because of magnetic field at the top of the HTS leads, the temperature of the cooler first stage must be kept below 55 K.

6. Some Concluding Comments

The three types of modules for the MICE cooling channel use a similar conductor. The peak current in the three coils varies from 210 A to 275 A. A common power supply is proposed for all of the magnets in the MICE cooling channel. A 300-A power supply will be used for the coupling coils and the focusing magnet (one power supply per magnet). The spectrometer solenoid will use three 300-A power supplies. There will be an individual 300-A power supplies for coils M1, M2 and the three coil spectrometer coil set (E1, Center and E2). Small ±60-A ±5 V power supplies will be used to tune coils E1 and E2 so that the field within the tracker will be uniform.

Because the MICE cooling channel solenoid magnets are unshielded, all of the MICE coil circuits (there are a total of eleven of them) will be coupled to every other coil circuit in MICE. The large coupling coils will couple strongly with the other coil circuits in the channel. Smaller magnet coils such as the focusing magnets, coils M1 and M2 will couple strongly with only their neighbors. As a result, the control of the power supplies for the MICE magnets will be an issue any time the currents in the magnet coils are changed.

The spectrometer magnet may be the largest superconducting magnet that has been kept cold using small coolers. The spectrometer magnet is cooled using three PT415 coolers. Because the heat load due to the leads is large, a single stage GM cooler will be added to cool the top of the HTS leads to below 55 K. Four PT-415 coolers have been tested in a test cryostat to demonstrate re-condensation and simultaneous first-stage cooling up to 55 W. The HTS-110 leads for this magnet are at 500 A at 64 K. Further testing is needed to see that the copper leads from 300 K are properly optimized to minimize the heat into the first stage from that source. Both magnets have had current in them to at least 70 percent of the peak current for the magnet.

The coupling solenoid is large in diameter, but its length is relatively short. This magnet will be cooled using two PT415 coolers. A single pair of copper leads carries the current into the magnet from 300 K. The rated current for the copper leads is 210 A. Because the field is high at the upper end of the HTS leads, it is important to keep the top of the leads below 55 K. The HTS-110 leads for this magnet are also rated at 500 A at 64 K. Because of the stray field, there isn't the option of using a single stage GM cooler to boost the cooling at the top of the HTS leads.

The focusing magnet is roughly the same diameter as the spectrometer solenoid, but the length and cold mass are less than 30 percent of that of the spectrometer solenoid. The cold mass support for this magnet must carry 900 kN in the axial direction. All of the other magnets only have to carry a maximum of 500 kN in the axial direction. The focusing magnet has two PT415 coolers for cooling the magnet, but there are two pairs of copper leads that are designed for 250 A. The cooler first stage temperature must be less than 55 K. Because of the stray field, there isn't the option of using a single stage GM cooler to boost the cooling the HTS leads.

The spectrometer solenoid is in a helium bath. The mandrel and the cover plate form a 190-liter helium tank. Because the axial forces on the spectrometer solenoid force the coils together, the stress in the longitudinal direction in the mandrel is low. Because the field within the spectrometer solenoid is relatively low (~4.5 T) and the coil ID = 516 mm, the hoop stresses in the mandrel are low. Thus the mandrel meets the requirements of the pressure vessel code when all stresses are present. The eight leads for the coil pass through the cold mass wall through specially designed feed through that are vacuum tight at 4 K. The four sets of quench protection diodes and the quench protection resistors are in the liquid helium bath. The cooler condenser condenses into the top of the helium bath in away that is similar to a typical MRI magnet.

The coupling coils and focusing coils have indirect cooling to helium in tubes that are welded in the cold mass forged cover plates. Even though the cool-down and magnetic stresses in the magnet mandrel are high, the magnet mandrel is not subject to the requirements of the pressure vessel code. The leads from the coils do not have to pass through a helium-tight feed through. The diodes are conduction cooled to the helium tanks attached to the cooling tubes. One must make sure that the bottom of the HTS leads and quench protection diodes are well tied to a 4 K region.

The re-condenser configuration for the coupling magnet is similar to the re-condenser configuration for the spectrometer solenoid (see Figure 5 configuration C). The final decision as to how re-condensation is done in the focusing magnet has not been made.

The spectrometer solenoids are scheduled to be delivered to the UK in 2010. The first of the focusing magnet will also be delivered later in 2010. The first MICE coupling magnet is supposed to be delivered at the same time as the second focusing magnet in 2011.

Acknowledgments

Most of the work in this report can be found in a series of MICE notes published from 2004 on. Access to the MICE notes is on the MICE web site at http://mice.iit.edu.

This work for this report was supported by the Lawrence Berkeley Laboratory and the Office of Science, United States Department of Energy, under the DOE contract DE-AC03-76SF00098. The work in China was also supported by the fund of cryogenics and superconductivity engineering technology innovation platform, the second phase of "985 Project" of Harbin Institute of Technology. The work in the United Kingdom was funded by the UK Sciences and Facilities Council.

References

[1] N. Holtkamp and D. Finley Eds., “A Feasibility Study of a Neutrino Source Based on a Muon Storage Ring,” FERMI-Pub-00/108E, (2000)

[2] R. B. Palmer, A. Sessler, A. Skrinsky, A. Tollestrup, et al, “Muon Colliders, “ Brookhaven National Laboratory Report BNL-62740, January 1996

[3] M. A Green and J. M. Rey, “Superconducting Solenoids for an International Muon Cooling Experiment,” *IEEE Transactions on Applied Superconductivity* **13**, No. 2 p 1373 (2003)

[4] Gregoire G, Ryckwaert G, Chevalier L et al, “MICE and International Muon Ionization Experiment Technical Reference Document,” http://mice.iit.edu 2002

[5] Vecsey G, “Supercritically Cooled Superconducting Muon Channel,” Preoceeding of the 4th International Cryogenic Engineering Conference, Eindhoven 24 –26 May 1972, IPC Science and Technology Press Ltd., United Kingdom (1972)

[6] Yang S Q, Baynham D E, Fabricatore P, et al, “The Physical Connection and Magnetic Coupling of the MICE Cooling Channel Magnets and the Magnetic Forces for Various Operating Modes,” *IEEE Transactions on Applied Superconductivity* **17**, No. 2, p 1225, (2007)

[7] Green M A, Witte H, Strauss B P, “The Inductive Coupling of the Magnets in MICE and its Effect on Quench Protection,” *IEEE Transactions on Applied Supercondutivity* **16**, No. 1, p 1304, (2006)

[8] Green M A, Yang S Q, Cobb J, et al, “The Effect of Magnetic Field on the Position of HTS Leads and the Cooler in the Services Tower of the MICE Focusing Magnet,” *IEEE Transactions on Applied Superconductivity* **18**, No. 2, p 1447, (2008)

[9] Green M A, “The Cost of Helium Refrigerators and Coolers for Superconducting Devices as a Fucntion of Cooling at 4 K,” *Advances in Cryogenic Engineering* **53**, p 872, AIP Press, Melville NY (2008)

[10] Green M A, “ Cooling MICE Magnets using Small Cryogenic Coolers,” MICE Note 109, http://mice.iit.edu, September 2004

[11] Green M A, “Cooling the MICE Liquid Hydrogen Absorbers using Small Cryogenic Coolers,” MICE Note 108, http://mice.iit.edu, September 2004

[12] Cryoech PT415 Cooler Specification Sheet, PT415 Cooler Brochure, Cryomech Inc. Syracuse NY, http://www.cryomech.com.

[13] Choi Y S, Painter T A, Kim D L, et al, “Helium Liquefaction by Cryocoolers for High Field Magnet Coolinjg,” *Proceedings of the International Cryocooler Conference* (2006)

[14] Green M A, Witte H, “The Use of Small Coolers in a Magnetic Field.” *Advances in Cryogenic Engineering* **53**, p 1299, AIP Press, Melville NY (2008)

[15] Wilson M N, “Superconducting Magnets,” Chapter 11, Oxford University Press, Oxford (1983)

[16] Kadin A M, Webber R J, and Gupta D, “Current Leads and Optimized Thermal Packaging for Superconducting Systems on Multi-stage Coolers,” *IEEE Transactions on Applied Superconductivity* **17**, No. 2, p 915, (2007)

[17] Cryomech Incorporated web site at http://www.cryomech.com.

[18] Green M A, "The Integration of Liquid Cryogen Cooling and Cryocoolers with Superconducting Electronics Systems," *Superconducting Science and Technology*, Vol. 16, No. 12, p 1349, (Dec. 2003).

[19] Green M A, How the Performance of a Superconducting Magnet is affected by the Connection between a Small Cooler and the Magnet, *IEEE Transactions on Applied Superconductivity* **16**, No. 1, p 1330, (2006)

[20] Green M A and Wang S T, “Tests of Four PT415 Coolers in the Drop-in Mode,” *Proceedings ICEC-22* in Seoul Korea, 21 to 25 July 2008, p 105 (2008)

[21] Green M A, “Re-condensation and Liquefaction of Helium and Hydrogen using Coolers,” to be published in *Advnaces in Cryogenic Engineering* **55**, AIP Press, Melville NY (2010), MICE Note 239, http://mice.iit.edu.

[22] Bravar U, "Coil Currents in MICE," MICE Note 88, http://mice.iit.edu, (2004)
[23] Fabricatore P, Farinon S, Perrelly M, Bravar U, and Green M A, "The Mechanical and Thermal Design for the Detector Solenoid Magnet System," *IEEE Transactions on Applied Superconductivty* **15**, No. 2, p 1255, (2005)
[24] Green M A, Virostek S P, Lau W W, and Yang S. K. "Preogress on the MICE Tracker Solenoid," *Proceedings of EPAC-06* Edinbourh UK, MICE Note 158, http://mice.iit.edu, (2006)
[25] Green M A, Chen C Y, Jiang T, et al, "Design Parameters for the MICE Tracker Solenoid," *IEEE Transactions on Applied Superconductivity* **17**, No. 2, p 1247 (2007).
[26] Green M A, Chen C Y, and Wang S T, "The Design and Construction of a Gradient Solenoid for a High Powered RF Cavity Experiment for the Muon Collider," *Institute of Physics Conference Series* **167**, p 1199, (2000)
[27] Wang S T, Wahrer R, Taylor C, et al, "The Design and Construction of the MICE Spectrometer Solenoids," *IEEE Transactions on Applied Superconductivity* **19**, No. 3, p 1348, (2009)
[28] Virostek S P, Green M A, Li D, et al, "Preliminary Test Results for the MICE Spectrometer Superconducting Solenods, *IEEE Transactions on Applied Superconductivity* **19**, No. 3, p 1364, (2009)
[29] Guo X L, Xu F Y, Wang L, et al,"Quench Protection for the MICE Cooling Channel Magnet," *IEEE Transactions on Applied Superconductivity* **19**, No. 3, p 1360, (2009)
[30] Green M A and Virostek S P, "The Dimensions and Number of Turns for the Spectrometer Solenoids As-built compared to the Original Design," LBNL-899E, MICE Note 207, http://mice.iit.edu, (2008)
[31] Green M A, Wu H, Wang L, et al, "AC Losses in the MICE Channel Magnets Is this a Curse or a Blessing?, LBNL-63804, MICE Note 195, http://mice.iit.edu, (2008)
[32] Green M A, "A Design of a Rapid Discharge Varistor System for the MICE Magnet Circuits," LBNL-900E, MICE Note 208, http://mice.iit.edu, (2008)
[33] Green M A, Yang S Q, Bravar U, et al, "The Mechanical and Thermal Design for the MICE Coupling Solenoid Magnet," *IEEE Transactions on Applied Superconductivity* **15**, No. 2, p 1279, (2005)
[34] Green M A, "The Effect of Extending the Length of the coupling Coils in a Muon Ionization Cooling Channel," *Proceeding of NyFact-07,* MICE Note 194, http://mice.iit.edu, (2007)
[35] Wang L, Xu F Y, Liu X K, et al, "Magnetic and Cryogenic Design of the MICE Coupling Solenoid System," *IEEE Transactions on Applied Superconductivity* **19**, No. 3, p 1344, (2009)
[36] Wang L, Liu X K, Xu F Y, et al, "Progress on the MuCOOL and MICE Coupling Coils," Proceeding of PAC-09, Vancouver Candada, MICE Note 240, http://mice.iit.edu, (2009)
[37] Wu H, Wang L, Liu X, K, "Structural Deisgn and Analysis for a Double-Band Cold Mass Support for the MICE Coupling Magnet," to be published in *Advances in Cryogenic Engineering* **55**, AIP Press, Melville NY, (2010)
[38] Green M A and Witte H, "Using High Temperature Superconducting Leads in a Magnetic Field," *Advances in Cryogenic Engineering* **53**, p 1251, AIP Press Melville NY, (2008)
[39] Xu F Y, Pan H, Wu H, et al, "Measurement of Resistance and Strength of Conductor Splices in the MICE Coupling Magnets, to be published in *Advances in Cryogenic Engineering* **55**, AIP Press, Melville NY (2010), MICE Note 257, http://mice.iit.edu
[40] Wang L, Pan H, Liu X K, et al, "Design and Construction of Test Coils for MICE Coupling Solenoid Magnet," *IEEE Transactions on Applied Superconductivity* **19**, No. 3 p 1340, (2009)
[41] Baynham D E, Bish P, Bradshaw T, et al, "A Liquid Cryogen Absorber for MICE," *Advances in Cryogenic Engineering* **51**, p 1068, (2006)
[42] Green M A, Chen J Y, and Wang S T, "A Test of a Superconducting Solenoid for the Mucool RF Experiment," *IEEE Transactions on Applied Supercondcutivity* **11**, No. 2, p 2296, (2001)

[43] Green M A, Carlson K A, Jurgens T G, et al, "A Test of the MUCOOL RF Solenoid at Fermilab," LBNL-46954, (2000)

[44] Yang S Q, Green M A, Barr G, et al, "The Mechanical and Thermal Design for the MICE Focusing Solenoid Magnet System," *IEEE Transactions on Applied Superconductivity* **15**, No. 2, p 1259, (2005)

[45] Green, M A and Witte H, "Quench Protection and Magnet Power Supply Requirements for the MICE Focusing and Coupling Magnets," MICE Note 114, http://mice.iit.edu, (2005)

[46] Yang S Q, Green M A, Lau W W, Senanayake R S, Strauss B, and Witte H, "The Cold Mass Support System and the Helium Cooling System for the MICE Focusing Solenoid," *IEEE Transactions on Applied Superconductivity* **17**, No. 2, p 1251, (2007)